

PACS numbers: 81.07.Pr, 84.60.Jt, 88.40.hj, 88.40.hm, 88.40.jn, 88.40.jp, 88.40.jr

## **Comparison between Organic and Perovskite Solar Cells: Concept, Materials and Recent Progress**

Ourida Ourahmoun

*Electronic Department,  
LATAGE Laboratory,  
Faculty of Electrical Engineering and Computing,  
University of Mouloud Mammeri of Tizi-Ouzou,  
B.P. 17 RP,  
15000 Tizi-Ouzou, Algeria*

This paper reports a comparison between the performances of photovoltaic cells based on perovskite materials and cells based on organic materials. Photovoltaic cells based on perovskite materials have better performance compared to cells based on organic materials. To study the influence of the donor–acceptor composition on the performance of the organic cells, three different active layers are used: P3HT:PCBM, P3HT:ICBA, PTB7:PC<sub>70</sub>BM. The organic cells are produced and characterized in the glove box. Results show that cells with P3HT:ICBA give the best yield of 5.58%. Perovskite solar cells are produced under atmospheric conditions and using similar structure and devices for producing organic cells. The yield obtained from the perovskite cells is better than the organic cells:  $\eta_{\text{perovskite}} = 8.81\%$ . A discussion on the degradation and stability of organic and perovskite solar cells is presented.

В цій статті повідомляється про порівняння між експлуатаційними якостями фотоелектричних елементів на основі перовскітних матеріалів і елементів на основі органічних матеріалів. Фотоелектричні елементи на основі перовскітних матеріалів мають кращі показники в порівнянні з елементами на основі органічних матеріалів. Для вивчення впливу донорно-акцепторного складу на продуктивність органічних елементів використовуються три різних активних шари: P3HT:PCBM, P3HT:ICBA, PTB7:PC<sub>70</sub>BM. Органічні елементи виробляються та характеризуються в рукавичній камері (для роботи зі шкідливими речовинами). Результати показують, що клітини з P3HT:ICBA дають кращий вихід 5,58%. Перовскітні сонячні елементи виробляються в атмосферних умовах і використовують аналогічну структуру та пристрої для виробництва органічних елементів. Вихід, одержаний з перовскітних елементів, ліпше, ніж з органічних елементів:  $\eta_{\text{perovskite}} = 8,81\%$ . Представлено обговорення щодо деградації та стабільності органічних і перовскітних сонячних елементів.

**Key words:** solar cells, perovskite, organic materials, structure, stability.

**Ключові слова:** сонячні елементи, перовскіт, органічні матеріали, структура, стабільність.

*(Received 18 March, 2020; in revised version, 5 August, 2020)*

## 1. INTRODUCTION

Organic and hybrid perovskite photovoltaic cells present the third generation of solar cells. Three types of cells can be distinguished in the third generation: polymer based solar cells; fullerene bulk heterojunction, small molecules based cells, and dye-sensitized hybrid cells (Grätzel cells). The production of organic solar cells can be done at low temperatures with a low manufacturing cost. In addition, the use of the mixtures in solution makes it possible to use active layers in the form of inks or paints, and consequently, these layers can cover large areas and be deposited on flexible substrates. Cells efficiency based on polymer blends: fullerene has increased steadily. The use of P3HT as donor and PCBM as acceptor polymers allowed a great advance in performances of P3HT:PCBM based cells; the efficiency exceeded 3%, then yields around 5% were shown in 2005 [1], to exceed finally 6% in 2007 [2]. Perovskite solar cells have attracted enormous interests in recent years with power conversion efficiencies (PCE) leaping from 3.8% in 2009 to the current world record of 22.1% [3]. Density functional theory (DFT) is used to investigate the structural, elastic, magnetic, and thermodynamic properties of the perovskite materials [4–8]. A conversion efficiency of 14.5% is achieved with cells based on perovskite materials in the structure FTO/Graphene/TiO<sub>2</sub>/perovskite/spiro-OMeTAD/AU [9].

Although organic solar cells have advantages over silicon-based photovoltaic cells because of their low cost, unlimited materials, their flexibility and ease of implementation, their low-temperature technology and the possibility of producing them over large areas, however, they have disadvantages: the operating time of these components is short, because of the low stability of the organic materials against moisture and oxygen [10, 11]. Perovskite preparation *via* simple and inexpensive solution processes demonstrates the immense potential of this thin-film solar technology to become a low-cost alternative to the presently commercially available photovoltaic technologies [12]. The major importance in the organic cells concern the synthesis of new low-gap electron-donor materials, allowing widening the absorption spectrum, and whose energy levels are better adapted than those P3HT to form mixtures with PCBM that may have higher open circuit voltage [13]. Doping of interfacial layers improves the performance of organic photovoltaic cells by reducing series resistance and increasing open

circuit voltage [14]. P3HT is the most donor material used in organic solar cells and PCBM is the most used acceptor material. Other donors and acceptors are used such as PTB7 and ICBA, respectively. PTB7:ICBA active layer is used to have higher yields,  $\eta = 7\%$  [15]. To improve cell stability, encapsulation systems can be used for the protection of cells against rapid ageing.

In this work, a state of the art of the recent results obtained on photovoltaic cells based on perovskite materials and on organic photovoltaic cells is presented. The results reported by literature show that the cells based on perovskite materials have better yields compared to the organic cells.

Three different active layers were made: P3HT:PCBM, P3HT:ICBA, and PTB7:PCBM. The results show that the efficiency of the organic cells depends on the type of materials used as active layer. The best yield is obtained in the case of the active layer P3HT:ICBA,  $\eta_{\text{P3HT:ICBA}} = 5.85\%$ . To compare the yields of the organic cells with those of the perovskite cells, a series of cells based on perovskite materials is realized. The structure of the cells realized is FTO/TiO<sub>2</sub>/perovskite/spiro-OMeTAD/Au; PCE of 8.81% is obtained. These results show that the yield of the perovskite photovoltaic cells is better than the yield of organic cells.

This study searches the reason for the difference between the performances of the two categories of the photovoltaic cells, some of the high-efficient devices from organic and perovskite devices are selected and presented.

A discussion on the stability of perovskite and organic cells is presented and solutions to improve the efficiency and the stability of the third generation solar cells are proposed.

## 2. COMPARISON BETWEEN PERFORMANCE OF PEROVSKITE SOLAR CELLS AND ORGANIC SOLAR CELLS

The schematic structures of both OSCs and PVSCs are fabricated based on two configurations called as normal and inverted. The organic solar cell contains an active layer sandwiched between two electrodes. In polymer solar cells, the active layer consists of a blend of conjugated polymers as a donor and an organic or inorganic conjugated polymer as acceptor to form an interpenetrating network. When incident photons are absorbed in the active layer, excitons are generated in the conjugated polymers. In normal structure, excitons are dissociated into free hole and electrons at the donor-acceptor interface. Subsequently, holes are transferred throughout the highest occupied molecular orbital (HOMO) of the polymer and collected at the anode, and electrons are transferred from the lowest unoccupied molecular orbital (LUMO) of the donor to the LUMO of the acceptor, and finally transported to

the cathode and collected. In contrast to the normal structure, after excitons dissociation, electrons and holes are transported to the transparent anode and metallic electrode, respectively. Both the hole transport layer and the electron transport layer are used to improve selectivity towards electrons or holes while blocking others.

The structure of the PVSCs can be divided into three categories: perovskite sensitized mesoporous or  $n-i-p$  structure, planar heterojunction structure, and inverted  $p-i-n$  structure. In all PVSCs configurations, after absorbing the incident photons by perovskite materials, excitons with a low binding energy are generated and dissociated into the free charge carriers without needing the acceptors. In mesoporous devices, halide perovskite is sandwiched between two contacts of anode and cathode, a thin film of compact  $\text{TiO}_2$  layer was deposited under the mesoporous layer. Further, an appropriate HTL such as spiro-OMeTAD is deposited on the top of the perovskite layer to improve the performance of the device. The planar heterojunction structure is more similar to the OSC. In this architecture, a perovskite material is sandwiched between ETL and HTL with a mesoporous scaffold. Two heterojunction are provided which are the junction between the absorber and HTL, and the junction between the absorber and ETL. Different types of materials are used as HTL, and a compact layer such as  $\text{TiO}_2$  layer is usually used as ETL. In the inverted devices, photogenerated electrons are collected in anode, Pedot:Pss and fullerene derivatives are commonly used as HTL and ETL, respectively. The advantages of this structure are as follow:  $\text{TiO}_2$  compact layer is replaced by organic ETL, which avoids the high-temperature annealing process, and the device structure is simpler. The stability of devices can be improved by removing  $\text{TiO}_2$  layer, which causes instability under UV light. The materials and process methods of this structure provide the fabrication of flexible PSCs, because flexible devices do not support high temperatures. The high-cost spiro-OMeTAD can be replaced by other organic materials. In both PVSCs and OSCs, ITO and FTO are widely used as anodes. Different metallic materials such as Al, Ag, Cu, and Au are used as cathodes in both PVSCs and OSCs.

The performance of perovskite solar cells or organic solar cells depends on several parameters such as the structure, the glass/FTO or glass/ITO substrates, the materials used for the active layer, the hole transport layer and the electron transport layer [16, 17], as shown in Table 1 and Table 2.

Comparison of the two categories reveals that their structures are almost similar. The main difference between them is related to the bulk heterojunction configuration of OSCs.

ETL and HTL in solar cells are commonly used for facilitating charge separation, charge transporting, and improving device stability. The materials are chosen according to their hole/electron

**TABLE 1.** Parameters of perovskite solar cells for different structures.

| Cells   | Structure of the perovskite cells   | $V_{oc}$ , V | $J_{sc}$ ,<br>mA/cm <sup>2</sup> | $FF$ , % | PCE, % | Ref. |
|---------|---|--------------|----------------------------------|----------|--------|------|
| Cell 1  | ITO/Pedot:Pss/MAPbI <sub>3</sub> /PCBM/Ag   | 0.981        | 19.65                            | 74       | 14.32  | [18] |
| Cell 2  | ITO/NiO <sub>x</sub> /MAPbI <sub>3</sub> /PCBM/Ag                                   | 1.101        | 21.28                            | 71       | 16.74  | [18] |
| Cell 3  | ITO/NiO <sub>x</sub> (undoped)/MAPbI <sub>3</sub> /<br>/bis-C <sub>60</sub> /Ag     | 1.01         | 21.38                            | 65       | 14.04  | [19] |
| Cell 4  | ITO/C-NiO <sub>x</sub> /MAPbI <sub>3</sub> /bis-C <sub>60</sub> /Ag<br>0.5 mol. %   | /            | 21.34                            | 71       | 15.48  | [19] |
| Cell 5  | 1.0 mol. %  | 1            | 21.47                            | 74       | 16.20  | [19] |
| Cell 6  | 2.5 mol. %  | 1.03         | 22.07                            | 74       | 16.82  | [19] |
| Cell 7  | 5 mol. %  | 1.04         | 22.46                            | 75       | 17.52  | [19] |
| Cell 8  | ITO/Zn-NiO <sub>x</sub> (5 mol. %)/MAPbI <sub>3</sub> /<br>/bis-C <sub>60</sub> /Ag | 1.04         | 19.83                            | 59       | 12.23  | [20] |
| Cell 9  | FTO/SnO <sub>2</sub> /perovskite/ <i>c</i> -Se/Au                                   | 0.86         | 19.89                            | 48.3     | 8.3    | [21] |
| Cell 10 | FTO/SnO <sub>2</sub> /perovskite/<br>/spiro-OMeTAD/Au                               | 1.12         | 21.06                            | 70.4     | 16.6   | [21] |
| Cell 11 | ITO/SnO <sub>2</sub> /MAPbI <sub>3</sub> /<br>/spiro-OMeTAD/Ag                      | 1.02         | 18.91                            | 50       | 9.68   | [24] |
| Cell 12 | ITO/Sb:SnO <sub>2</sub> /MAPbI <sub>3</sub> /HTM/Au                                 | 1.06         | 22.5                             | 67.8     | 16.2   | [24] |
| Cell 13 | FTO/Nb <sub>2</sub> O <sub>5</sub> /perovskite/<br>/spiro-OMeTAD/Au                 | 1.04         | 21.12                            | 67       | 14.78  | [27] |

transport properties, processing methods, and their energy levels. Their energy levels should be well matched with the energy levels of the active layer materials.

Pedot:Pss is a promising HTL for both organic and perovskite solar cells. Consequently, inorganic HTLs were attended as more stable and low cost materials to replace organic ones. Moreover, inorganic HTLs have higher mobilities than the organic ones.

All conjugated polymers employed as HTLs in PVSCs are the polymers utilized as donors or absorbers in OSCs. The inorganic HTLs in both categories are common.

The general aspects of the fabrication methods of these two types of solar cells are similar. The methods used are spin coating, printing, and roll-to-roll. For PVSCs, perovskite layer morphology and crystallization are more dependent on the process parameters such as temperature, composition, solvents, atmosphere conditions, and time of deposition than morphology of polymers. In the case of OSCs, achieving interpenetrating network morphology with a domain size between 10 and 20 nm has still remained as a challenge. The high toxicity of lead based perovskite materials as usual material in PVSCs is one of the most important challenges in this area.

**TABLE 2.** Parameters of some organic photovoltaic cells.

| Cells   | Structure of the organic cell   | $V_{OC}$ , V | $J_{sc}$ , mA/cm <sup>2</sup> | $FF$ , % | PCE, % | Ref. |
|---------|---|--------------|-------------------------------|----------|--------|------|
| Cell 14 | ITO/Pedot:PSS/MoO <sub>3</sub> /<br>/PDBTDPTz:PC <sub>71</sub> BM/PFN-Br/Al | 0.87         | 9.04                          | 52.3     | 4.11   | [28] |
| Cell 15 | ITO/ZnO/P3HT:PCBM/MoO <sub>3</sub> /Ag                                      | 0.64         | 8.82                          | 61       | 3.46   | [29] |
| Cell 16 | Insulated steel/Al/P3HT:<br>:PCBM/MoO <sub>3</sub> /Au                      | 0.6          | 11.2                          | 43       | 2.89   | [30] |
| Cell 17 | ITO/PETE/PC <sub>70</sub> BM:PTB7/MoO <sub>x</sub> /Al                      | 0.758        | 14.2                          | 69.9     | 7.52   | [31] |
| Cell 18 | ITO/Pedot:PSS/P3HT:ICBA/Ca/Al   | 0.81         | 6.51                          | 61       | 3.19   | [32] |
| Cell 19 | ITO/ZnO/P3HT:ICBA/Pedot:Pss/Ag  | 0.81         | 8.9                           | 48       | 3.5    | [33] |
| Cell 20 | ITO/Pedot:Pss/H <sub>3</sub> BO <sub>3</sub> /P3HT:<br>:PCBM/Al             | 0.62         | 7.57                          | 46.9     | 2.14   | [34] |

The photovoltaic performances of some perovskite solar cells are presented in Table 1. The doping of the hole transport layer improves the performances of perovskite solar cells. Nickel oxide is used as hole transport layer. High-quality solution processed NiO<sub>x</sub> thin films were prepared by optimizing ethylenediamine (EDA) concentration from 0 to 10% in the NiO<sub>x</sub> precursor solution [18]. With the proper EDA content 5%, the electrical resistivity could be decreased.

By applying this NiO<sub>x</sub> as HTL for planar perovskite solar cells a PCE of 16.7% is obtained, cell 2. Whereas, device made with EDA free NiO<sub>x</sub> showed 13.9%. For cells using Pedot:Pss as HTL, the PCE is about 14.3% (cell 1). In addition, the effect of cobalt doping NiO<sub>x</sub> (Co-NiO<sub>x</sub>) on the photovoltaic performance of planar heterojunction perovskite cells was reported in the inverted structure [19]. It is noted that better charge transport and low energy loss is expected with devices with Co-NiO<sub>x</sub> because of the well-matched energy levels to CH<sub>3</sub>NH<sub>3</sub>PbI<sub>3</sub> (MAPbI<sub>3</sub>) than the pristine NiO<sub>x</sub>.

The PCE of the devices were optimized by varying the cobalt doping concentration from 0.5 mol.% to 5 mol.% to show the parameters of perovskite solar cells using pristine NiO<sub>x</sub> and Co-NiO<sub>x</sub> as HTL. The device with undoped NiO<sub>x</sub> (cell 3) delivers PCE of 14.04% with open circuit voltage of 1.01 V, a short current density of 21.38 mA/cm<sup>2</sup>, and a fill factor of 65%. The device using Co-NiO<sub>x</sub> as HTL exhibited an improved PCE of 15.48% (cell 4), 16.20% (cell 5) and 16.82% (cell 6) for a cobalt concentration 0.5, 1.0, and 2.5 mol.%, respectively. As cobalt concentration increased to 5 mol.%, the device (cell 7) showed 17.5% with a  $V_{OC}$  of 1.04 V,  $J_{sc}$  of 22.46 mA/cm<sup>2</sup> and  $FF$  of 75%. Co-NiO<sub>x</sub> reduced internal resistance and charge leakage of PVSCs [19].

Pristine NiO<sub>x</sub> possesses unsatisfactory electrical properties such as high surface trap density and low electrical conductivity, which could

deteriorate the device performance. Zn doped  $\text{NiO}_x$  is also employed as HTL in planar heterojunction, because Zn forms highly crystalline oxide materials. 5% Zn doped devices (cell 8) achieved PCE up to 12.23% with improvement of  $V_{\text{OC}}$  by 4%,  $J_{\text{sc}}$  by 16.7% and  $FF$  by 8.9% as compared to the undoped  $\text{NiO}_x$ . Zn-doped  $\text{NiO}_x$  as hole transport layers are promising material, with which to construct efficient and stable perovskite solar cells [20]. Crystalline selenium (*c*-Se) prepared by thermal evaporation by annealing at low temperature was used as inorganic HTL for the planar PVSCs (cell 9) in the device structure FTO/ $\text{SnO}_2$ /perovskite/*c*-Se/Au [21].

$\text{TiO}_2$  is demonstrated to be the best choice as an electron transport layer in PVSCs. Because of its inferior mobility and high crystallization temperatures (400–500°C), its applications are limited to glass substrates only. Tin oxide ( $\text{SnO}_2$ ) has advantages over  $\text{TiO}_2$  and ZnO through its superior inherent features such as wide gap about 3.6 eV, and low processing temperature (< 100°C). These characteristics make it a viable alternative ETL in PVSCs fabricated on flexible polymer based substrates. The PCE of up to 21% has been achieved for ETL based pure  $\text{SnO}_2$ , its composite with ZnO or PCBM and doped forms synthesized at low temperature [22]. Sb-doping  $\text{SnO}_2$  significantly enhanced the photovoltaic performance of PVSCs by increasing the  $FF$  and  $V_{\text{OC}}$ , and reducing photocurrent hysteresis [24]. The incorporation of Mo dopant within the pure  $\text{SnO}_2$  enhances the conductivity and facilitates the photogenerated charge carriers. The PCE for pure  $\text{SnO}_2$  and  $\text{SnO}_2$ :Mo based PVSCs was about 8.74% and 10.52%, respectively [25]. Reduced cerium oxide  $\text{CeO}_x$  is used also as ETL in PVSCs [26]. Niobium oxide ( $\text{Nb}_2\text{O}_5$ ) has been used as electron transport layer for PVSCs (cell 14) due to its excellent optical transmittance and similar Fermi level with  $\text{TiO}_2$  [27].

Table 2 gives some results obtained recently on organic photovoltaic cells. Pedot:Pss is the most material used as HTL in OSCs. However, it suffers from acidity and hygroscopicity which results in degraded efficiency of the OSCs. Semiconducting metal oxides such as  $\text{MoO}_3$ ,  $G\text{-MoO}_3$ ,  $\text{V}_2\text{O}_5$ ,  $\text{WO}_3$ , NiO,  $\text{RuO}_2$  are used as alternatives to Pedot:Pss due to their advantages of excellent optical and electrical properties, which can achieve high efficiency. Organic devices based on BDTDPTz:PC<sub>71</sub>BM as active (cell 14) layer exhibits PCE of 4.11%,  $V_{\text{OC}}$  of 0.87 V,  $J_{\text{sc}}$  [ $\text{mA}/\text{cm}^2$ ] of 9.04% and  $FF$  of 52.3% [28]. Buffer layers take an important parameter, which enhances performance of OSCs and PVSCs. Various materials have been used as ETL in OSCs such as zinc oxide (ZnO), aluminium-doped ZnO (AZO), zinc–tin oxide (ZTO), indium–zinc oxide (IZO), titanium oxide ( $\text{TiO}_2$ ),  $\text{Cs}_2\text{CO}_3$ ,  $\text{CsF}_2$ , PbO, and CdS [29]. The use of ICBA as an acceptor and PTB7 as a donor in OSCs improves performance [31–33]. Doping of Pedot:Pss by boric acid ( $\text{H}_3\text{BO}_3$ ) improves the efficiency of the organic cells. The best yield is

obtained for a concentration of 1.25 mg/ml of boric acid in the Pedot:Pss (cell 20); the PCE achieved is about 2.14% [34]. Inorganic HTL are used because the hygroscopic nature of Pedot:Pss degrades the ITO electrode and decomposes the perovskite absorber layer. Other factors affect the parameters of PVSCs and OSCs, such as thermal annealing and additives incorporated into active layers. Both organic materials and perovskite materials are deposited in solution by the spin-coater device. This allows the realization of large area cells at low cost.

### 3. EXPERIMENTAL

#### 3.1. Production of Organic Solar Cells

The cells produced are composed of a transparent glass ITO cathode. The cathode is covered with an electron transport layer based on zinc nanoparticles (ZnO (NP)), then with the active layer consisting of a mixture of conjugated polymers. Three different active layers are used: P3HT:PCBM, P3HT:ICBA, and PTB7:PC<sub>70</sub>BM. To improve the transport of holes a layer of PEDOT (F010) is deposited on the active layer and finally silver electrode is deposited as anode. In inverted photovoltaic cells, the electrons are collected by the transparent electrode, and the holes are collected by the upper metal electrode. The photoactive layers, the electron transport layers, and the hole transport layers are deposited using spin-coating device. The silver anode is evaporated under vacuum at  $10^{-6}$  mbar using thermal evaporation device *r*. Finally, the structure of the realized cells is shown in Fig. 1.

#### 3.2. Production of Perovskite Solar Cells

The cells produced are composed of a transparent glass FTO cathode. This cathode is covered with an electron transport layer based on TiO<sub>2</sub>,

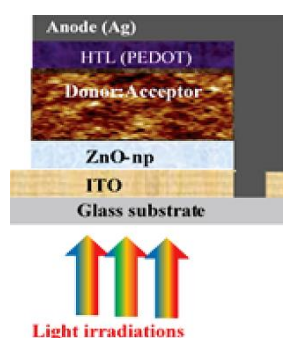


Fig. 1. Structure of the organic solar cells realized.

then with the photoactive layer consisting of a perovskite material. To improve the transport of holes, HTL is deposited on the active layer and finally, the gold is evaporated as anode. The final structure is FTO/TiO<sub>2</sub>/CH<sub>3</sub>NH<sub>3</sub>PbI<sub>3-x</sub>Cl<sub>x</sub>/spiro-OMeTAD/Au. The perovskite absorber layers, the electron transport layers, and the hole transport layers are deposited using spin-coating device. The gold anode is evaporated under vacuum at 10<sup>-6</sup> mbar. The structure of the PVSCs realized is shown in Fig. 2.

#### 4. RESULTS AND DISCUSSIONS

The structure of the organic cells realized is Glass/ITO/ZnO(NP)/donor:acceptor/PEDOT (F010)/Ag. The performance of the cells is given according to the type of the donor:acceptor mixture. The  $J(V)$  characteristics are measured using solar simulator.

The results on the characteristics  $J(V)$  presented in Fig. 3 are those

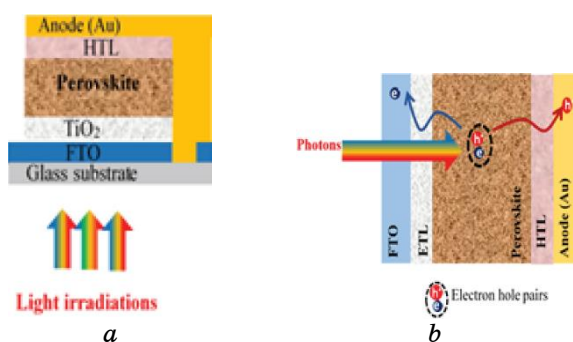


**Fig. 2.** (a) Structure of the perovskite solar cells realized; (b) photogenerated of charges in the PVSCs.

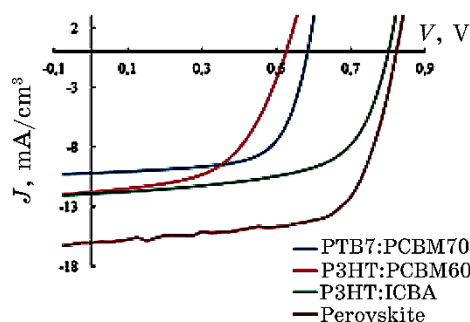


**Fig. 3.** Comparison between  $J(V)$  characteristics of organic solar cells and perovskite solar cells.

**TABLE 3.** Comparison between performances of organic cells and perovskite cells realized in this work.

| Cells  | Photovoltaic cell                                | $V_{OC}$ , V | $J_{sc}$ , mA·cm <sup>-2</sup> | $FF$ , % | $\eta$ , % |
|--------|--|--------------|--------------------------------|----------|------------|
| Cell A | ITO/ZnO/P3HT:PCBM <sub>60</sub> /PEDOT(F010)/Ag  | 0.52         | 11.69                          | 55       | 3.32       |
| Cell B | ITO/ZnO/PTB7:PCBM <sub>70</sub> /PEDOT(F010)/Ag  | 0.57         | 10.09                          | 68       | 3.89       |
| Cell C | ITO/ZnO/P3HT:ICBA/PEDOT(F010)/Ag                 | 0.79         | 11.83                          | 63       | 5.85       |
| Cell D | FTO/TiO <sub>2</sub> /perovskite/spiro-OMeTAD/Au | 0.81         | 16                             | 67       | 8.81       |

of the cells with the best efficiency for each of active layer. The electrical parameters of the cells for the different active layers are shown in Table 3. The results show that in the case of organic cells; cell with P3HT:ICBA gives the best yield compared to cell with P3HT:PCBM or cell with PTB7:PCBM;  $\eta_{P3HT:PCBM} = 3.32\%$  (Cell A),  $\eta_{PTB7:PCBM} = 3.89\%$  (Cell B) and  $\eta_{P3HT:ICBA} = 5.85\%$  (Cell C). In the case of the perovskite solar cells (Cell D), the yield achieved  $\eta_{perovskite} = 8.81\%$ . Photovoltaic cells based on perovskites materials have the best efficiency this due to the improvement of the open circuit voltage  $V_{OC}$  and the increase of the short circuit current  $J_{sc} = 16$  mA/cm<sup>2</sup> as is mentioned in Table 3.

The photovoltaic performance of a solar cell depends on the optical and electrical properties, and the morphology of the absorber layers. The absorption coefficient of perovskite materials (around  $10^5$  cm<sup>-1</sup>) is higher than the absorption coefficient of organic materials ( $10^4$  cm<sup>-1</sup>).

The excitons binding energy ( $E_b$ ) plays an important role on the generation and recombination of charges.  $E_b$  of the conjugated polymers is between 0.5 to 1.2 eV, while in perovskite materials,  $E_b$  is between 2–100 meV. The diffusion length of excitons in organic materials is between 5 and 10 nm. In PVSCs, the diffusion length of charge carriers is about 10  $\mu$ m. Perovskite have highly crystalline structure, the transport of charge is ambipolar (both electrons and hole participate on the conduction), and the mobility of the charge carriers of perovskite materials is higher than the mobility of charge carriers of organic materials, because organic materials have a semi-crystalline structure.

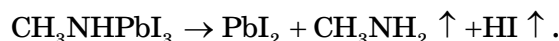
## 5. STABILITY OF PEROVSKITE AND ORGANIC SOLAR CELLS

Perovskite and organic materials are sensitive to atmospheric conditions and especially to humidity. To improve the performance of photovoltaic cells and protect cells from degradation, an encapsulation is required. The encapsulation is used to protect the cells against the penetration of O<sub>2</sub> and H<sub>2</sub>O into the cells and to improve their efficiency and stability. Significant enhancement in the device lifetime is observed for devices stored under ambient humidity and temperature conditions

compared to non-encapsulated control device. Partially encapsulated devices retained more than 80% of their initial PCE over 400 h, with a rapid performance loss after 400h. The devices encapsulated, using complete encapsulation architecture, were stable over the duration of the storage time (500 h) [35].

The stability of the PVSCs was improved by employing Norland Optical Adhesive and Polyethylene Terephthalate (NOA/PET) encapsulation. Solar cells encapsulated with NOA/PET show stability under approximately 540 h exposure to moisture. However, the non-encapsulated solar cells are immediately deteriorated in PCE [36].

In addition, the typically used spiro-OMeTAD hole transport layer, and additives limit long-term stability. The morphology of spiro-OMeTAD can cause perovskite solar cells to degrade. The macro- and micropinholes in spiro-OMeTAD film form channels that facilitate the inward and outward diffusion of gas species. A pinhole free spiro-OMeTAD can enhance stability. The Au electrode can cause degradation when Au atoms diffuse into the spiro-OMeTAD and perovskite layers under high temperatures, which deteriorates performance. Low-cost Ag electrode reacts with perovskite degrading its performance even in an encapsulated device. Exposure to high temperatures also causes degradation of the perovskite layer. The decomposition of the perovskite under high temperature is given by the following equation:



To improve stability, it is good to use passivated structure by replacing Ag and gold with Al/MoO<sub>3</sub> electrodes in order to reduce trap density and enhance diffusion length.

To further develop advanced fabrication process, minimizing material costs and lessening environment impacts, the following actions may be considered: (i) avoid the use of ITO or FTO, which, from its high cost, has high environment impact (CO<sub>2</sub> emissions) and is the cause of lower efficiencies due to increased resistance, also indium is a rare material and is expensive; (ii) avoid the use of Au or Ag electrodes (carbon electrodes are promising alternatives); (iii) HTL free perovskite solar cells are desirable; (iv) development of recycling technology; (v) development of less-toxic solvent; encouraging of lead free perovskite; (vi) develop new alternative materials that will make this technology more attractive to industry.

Another solution to enhance the performance of the cells is to replace organic electron/hole transport layers with inorganic materials. And to use materials with complementary optical absorption spectra to build a tandem solar cell, since tandem solar cells can harvest more photons and improve the open circuit voltage of the devices thus improving the efficiency.

## 6. CONCLUSION

Two categories of third generation solar cells including OSCs and PVSCs were introduced comparatively. Photovoltaic cells based on perovskite materials have better performance compared to cells based on organic materials. Several parameters affect the performance of perovskite devices such as active layers, electron transport layers, hole transport layers, and electrodes. Inorganic oxide films used as HTL or ETL display better environmental stability than their organic counterparts. To improve the performance of the cells, the inorganic HTL layers were doped.

In the experimental part of this work, in the case of perovskite cells with structure FTO/TiO<sub>2</sub>/perovskite/spiro-OMeTAD/Au, a better yield of 8.81% is obtained. The best yield obtained in the case of the realized organic solar cells is of 5.85% for the active layer P3HT:ICBA because of the low-band gap of the acceptor ICBA.

Photovoltaic cells are unstable in the presence of moisture and oxygen. The proposed solution to improve stability of these devices is encapsulation, and to improve environmental impact lead-free perovskite materials are required.

## REFERENCES

1. W. Ma, C. Yang, X. Gong, K. Lee, and A. J. Heeger, *Advanced Functional Materials*, **15**, No. 10: 1617 (2005).
2. K. Kim, J. Liu, M. A. Namboothiry, and D. L. Carroll, *Applied Physics Letters*, **90**, No. 16: 163511 (2007).
3. M. Saliba, T. Matsui, J. Y. Seo, K. Domanski, J. P. Correa-Baena, M. K. Nazeeruddin, and M. Grätzel, *Energy & Environmental Science*, **9**: 1989 (2016).
4. R. Arar, T. Ouahrani, D. Varshney, R. Khenata, G. Murtaza, D. Rached, and A. H. Reshak, *Materials Science in Semiconductor Processing*, **33**: 127 (2015).
5. K. Bidai, M. Ameri, S. Amel, I. Ameri, Y. Al-Douri, D. Varshney, and C. H. Voon, *Chinese Journal of Physics*, **55**: 2144 (2017).
6. F. Litimein, R. Khenata, A. Bouhemadou, Y. Al-Douri, and S. B. Omran, *Molecular Physics*, **110**: 121 (2012).
7. N. Moulay, M. Ameri, Y. Azaz, A. Zenati, Y. Al-Douri, and I. Ameri, *Materials Science-Poland*, **33**: 402 (2015).
8. A. H. Reshak, M. S. Abu-Jafar, and Y. Al-Douri, *Journal of Applied Physics*, **119**: 245303 (2016).
9. J. Bouclé and N. Herlin-Boime, *Synthetic Metals*, **222**: 3 (2016).
10. A. Rivaton, S. Chambon, M. Manceau, J. L. Gardette, N. Lemaotre, and S. Guillerez, *Polymer Degradation and Stability*, **95**, No. 3: 278 (2010).
11. M. Jørgensen, K. Norrman, and F. C. Krebs, *Solar Energy Materials and Solar Cells*, **92**, No. 7: 686 (2008).
12. A. Jena, A. Kulkarni, and T. Miyasaka, *Chemical Reviews*, **119**: 3036 (2019).

13. N. Blouin, A. Michaud, D. Gendron, S. Wakim, E. Blair, R. Neagu-Plesu, and M. Leclerc, *Journal of the American Chemical Society*, **130**: No. 2: 732 (2008).
14. A. Barbot, B. Lucas, and C. Di Bin, *Organic Electronics*, **15**, No. 4: 858 (2014).
15. M. Raïssi, S. Vedraïne, R. R. Garuz, T. Trigaud, and B. Ratier, *Solar Energy Materials and Solar Cells*, **160**: 494 (2017).
16. S. D. Stranks, G. E. Eperon, G. Grancini, C. Menelaou, M. J. Alcocer, T. Leijtens, and H. J. Snaith, *Science*, **342**: No. 6156: 341 (2013).
17. E. Edri, S. Kirmayer, S. Mukhopadhyay, K. Gartsman, G. Hodes, and D. Cahen, *Nature Communications*, **5**: 3461 (2014).
18. S. Yoon and D. W. Kang, *Ceramics International*, **44**, No. 8: 9347 (2018).
19. J. H. Lee, Y. W. Noh, I. S. Jin, S. H. Park, and J. W. Jung, *Journal of Power Sources*, **412**: 425 (2019).
20. J. H. Lee, Y. W. Noh, I. S. Jin, and J. W. Jung, *Electrochimica Acta*, **284**: 253 (2018).
21. Y. Di, Q. Zeng, C. Huang, D. Tang, K. Sun, C. Yan, and Y. Lai, *Solar Energy Materials and Solar Cells*, **185**: 130 (2018).
22. Q. Wali, Y. Iqbal, B. Pal, A. Lowe, and R. Jose, *Solar Energy Materials and Solar Cells*, **179**: 102 (2018).
23. X. Liu, K. W. Tsai, Z. Zhu, Y. Sun, C. C. Chueh, and A. K. Y. Jen, *Advanced Materials Interfaces*, **3**, No. 13: 1600122 (2016).
24. Y. Bai, Y. Fang, Y. Deng, Q. Wang, J. Zhao, and X. Zheng, and J. Huang, *ChemSus Chem.*, **9**, No. 18: 2686 (2016).
25. J. Bahadur, A. H. Ghahremani, B. Martin, T. Druffel, M. K. Sunkara, and K. Pal, *Organic Electronics*, **67**: 159 (2019).
26. R. Pandey, A. P. Saini, and R. Chaujar, *Vacuum*, **159**: 173 (2019).
27. Y. Guo, J. Tao, J. Jiang, J. Zhang, J. Yang, S. Chen, and J. Chu, *Solar Energy Materials and Solar Cells*, **188**: 66 (2018).
28. K. Wang, Z. Xu, Y. Geng, H. Li, C. Lin, L. Mi, and Y. Li, *Organic Electronics*, **64**: 54 (2019).
29. S. Banerjee, S. K. Gupta, A. Singh, and A. Garg, *Organic Electronics*, **37**: 228 (2016).
30. L. S. Pali, S. K. Gupta, and A. Garg, *Solar Energy*, **160**: 396 (2018).
31. R. Sharma, H. Lee, V. Gupta, H. Kim, M. Kumar, C. Sharma, and D. Gupta, *Organic Electronics*, **34**: 111 (2016).
32. A. Konkin, U. Ritter, P. Scharff, M. Schrödner, S. Sensfuss, A. Aganov, and G. Ecke, *Synthetic Metals*, **197**: 210 (2014).
33. T. Schneider, S. Gärtner, B. Ebenhoch, J. Behrends, and A. Colsmann, *Synthetic Metals*, **221**: 201 (2016).
34. Ö. Yagci, S. S. Yesilkaya, S. A., Yüksel, F. Ongül, N. M. Varal, M. Kus, and O. Icelli, *Synthetic Metals*, **212**: 12 (2016).
35. H. C. Weerasinghe, Y. Dkhissi, A. D. Scully, R. A. Caruso, and Y. B. Cheng, *Nano Energy*, **18**: 118 (2015).
36. B. J. Kim, J. H. Jang, J. Kim, K. S. Oh, E. Y. Choi, and N. Park, *Materials Today Communications*, 100537 (2019).